JOURNAL OF MATERIALS SCIENCE **40** (2005) 1869–1881

Enthalpy relaxation and free volume changes in aged styrene copolymers containing a hydrogen bonding co-monomer

E.-A. McGONIGLE, J. M. G. COWIE*, V. ARRIGHI
Department of Chemistry, School of Engineering and Physical Sciences, Heriot-Watt University, Riccarton Campus, Edinburgh, EH14 4AS

R. A. PETHRICK
Department of Pure and Applied Chemistry, Strathclyde University, 295 Cathedral Street, Glasgow, G1 1XL

Enthalpy relaxation of polystyrene (PS) and four modified polystyrene copolymers containing co-monomers capable of forming hydrogen bonds of different strengths is described. Values of enthalpy lost ($\Delta H(T_a, t_a)$) were calculated from experimental data plotted against log (t_a) and modelled using the Cowie-Ferguson (CF) semi-empirical model. This gives a set of values for three adjustable parameters, $\Delta H_\infty(T_a)$, log (t_c) and β. Each of the parameters defines the relaxation process, which was found to be sensitive to changes in hydrogen bond strength. The introduction of hydrogen bonding causes a slower relaxation compared with PS, with a greater overall enthalpy lost measured for the all the copolymers except the styrene-co–4-hexafluoro-2-hydrox isopropyl styrene (SHFHS). Interestingly, the free volume of this copolymer measured using Positron Annihilation Lifetime Spectroscopy (PALS) was greater than that of PS. Furthermore, the SHFHS copolymer had the lowest change in heat capacity (ΔC_p) of any of the systems on passing through the glass transition, T_g. All experiments indicate that the enthalpy lost by the fully relaxed glass ($\Delta H_\infty(T_a)$) is less than the theoretical amount possible on reaching the state defined by the equilibrium liquid enthalpy line ($\Delta H_{max}(T_a)$). The results are discussed with reference to the strength of interaction and free volume.

1. Introduction

Amorphous polymers, at temperatures below their glass transition, T_g, are in a non-equilibrium state [1]. They are said to be '*solidified supercooled liquids*' with an excess volume, enthalpy and entropy relative to the equilibrium state. Physical ageing or structural relaxation is the process whereby amorphous materials in the glassy state approach a state of thermodynamic equilibrium as a result of localised relaxation processes [2]. Physical ageing can be detected through the time evolution of thermodynamic properties such as the specific volume or enthalpy, as well as the mechanical, dielectric or other physical properties [1]. An appreciation of physical ageing is of technological importance because after ageing, a material may have changed dimensions and may not perform to its original specification.

Copolymerisation is frequently used to produce new materials with properties somewhere between those of the parent homopolymers. Copolymerising styrene with the co-monomers illustrated in Fig. 1 produces copolymers which are capable of forming hydrogen bonds. The hydroxyl group in the para-position of the aromatic ring can act as both a proton donor and acceptor, forming self-associated hydrogen bonds in the copolymers or inter-associated hydrogen bonds in blends with polymers with a proton accepting group such as poly(vinyl methyl ether) (PVME) [3].

In copolymers of styrene (S) with 4-(2-hydroxyethyl) styrene (HES), 4-(1,1,1-trifluoro-2-hydroxyethyl) styrene (TFHS) and 4-(hexafluoro-2-hydroxy isopropyl) styrene (HFHS), the hydrogen bond formation will be influenced by inductive effects of the groups adjacent to the alcohol. Hydrogen bond formation in copolymers of styrene with 4-hydroxystyrene (HS) will be influenced by the strong acidity of the phenol groups resulting from resonance effects with the benzene ring. A previous work in this group has shown that in blends of these modified copolymers with PVME, the hydrogen bond strength increases in the order (a) < (b) < (c) < (d) [4]. It is, therefore, of interest to establish if the same hierarchy of hydrogen bond strength exists in the copolymers. Furthermore, we are

*Author to whom all correspondence should be addressed.

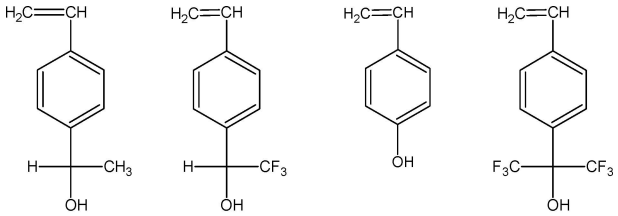

Figure 1 Modified polystyrene systems: (a) 4-(2-hydroxyethyl) styrene [HES], (b) 4-(1,1,1-trifluoro-2-hydroxyethyl) styrene [TFHS], (c) 4-hydroxystyrene [HS], (d) 4-(hexafluoro-2-hydroxy isopropyl) styrene [HFHS].

interested in the effects the hydrogen bonds formed in these copolymers will have on physical ageing.

In this investigation, physical ageing will be studied by following enthalpy relaxation or recovery, which is easily measured by differential scanning calorimetry (DSC). The technique has been proven to yield useful data on the long-term physical ageing process from short-term measurements [1]. The enthalpy relaxation data will be analysed using the semi-empirical Cowie-Ferguson (CF) model, described in Equations 1 and 2 [5].

$$\Delta H(T_a, t_a) = \Delta H_\infty[1 - \Phi(t_a)] \quad (1)$$

where,

$$\Phi(t_a) = \exp[-(t/t_c)^\beta] \quad (2)$$

is the Williams-Watts relaxation function. β defines the width of the relaxation time spectrum and t_c is a characteristic time ($\phi(t_c) = 1/e$) i.e. a kinetic parameter. The parameters $\Delta H_\infty(T_a)$, β and log (t_c) are obtained from a nonlinear least-squares curve-fitting algorithm.

This model attempts to predict the enthalpy lost on annealing to equilibrium ($\Delta H_\infty(T_a)$) by curve-fitting to experimental enthalpy data accumulated at various ageing temperatures after a range of ageing times ($\Delta H(T_a, t_a)$). These values are calculated from the experimental heat capacity, C_p, data obtained from the DSC measurements.

The model has been applied to a number of polymeric systems, including poly(methyl methacrylate) (PMMA) [5], poly(vinyl acetate) (PVAc) [6], poly(vinyl methyl ether) (PVME), several para-substituted polystyrenes [7] and styrene-maleic anhydride (SMA) copolymers [8]. The model has also been used to investigate the ageing of polymer blends such as poly(styrene) (PS)/PVME [9], PHS/PVME [10] and SMA/PMMA [11]. In a subsequent publication, the heat capacity data presented in this paper will be reassessed using a configurational entropy model proposed by Gómez and Monleón [12, 13].

The importance of free volume on molecular motion and physical properties in polymeric materials has long been recognised. Positron Annihilation Lifetime Spectroscopy (PALS) has emerged as a convenient means of measuring free volume properties of polymeric materials [14]. The sensitivity of the PALS in determining free volume hole properties is due to the unique localisation of the e^+ and positronium species (Ps, a bound state between an electron and positron) in areas of low electron density such as free volume in polymers. The observed lifetime, τ_3, of the triplet state of Ps i.e. orthopositronium (oPs), can be directly related to free volume hole size and the corresponding intensity, I_3, can be related to the number of free volume holes in the material.

In this paper we present enthalpy relaxation data on modified styrene copolymers. The discussion will be restricted to copolymers having 20–25 mol% of the co-monomers shown in Fig. 1. The resulting copolymers contain strong specific hydrogen bonding interactions due to self-association of the hydroxyl group. One of the incentives for studying the ageing of these copolymers is that physical ageing of polymeric materials with specific interactions, such as hydrogen bonds has not received much attention in the literature. Hydrogen bonds are essentially thermo-reversible crosslinks, which could potentially give rise to low ageing materials with high dimensional stability and low segmental motion. Furthermore, before examining enthalpy relaxation behaviour of blends of these copolymers with PVME, it is necessary to understand the physical ageing of the component copolymers. The ageing data will be discussed with reference to changes in the hydrogen bonding network and free volume resulting from changes in the co-monomer component. Infrared spectroscopy and PALS will be implemented to assist with final objective.

2. Experimental

2.1. Preparation of monomers

Styrene (S) and 4-acetoxystyrene (AS) monomers were obtained from the Aldrich Chemical Company and inhibitors removed by standard techniques prior to use.

Preparation of 4-vinyl-acetophenone (VA) involved pyrolysis of poly(vinylacetophenone), which was prepared by the complete acylation of polystyrene (PS) according to the procedure of Kenyon and Waugh [15]. A few crystals of hydroquinone were added to the crude distillate from the pyrolysis, and then distilled under reduced pressure (1.6×10^{-1} mbar) to give the desired product.

The synthesis of 4-vinyl-trifluoro-acetophenone (VTA) from 4-chlorostyrene using a Grignard reaction with trifluoroacetic acid in dry tetrahydrofuran (THF), was as described by Cheng and Pearce [16]. The crude product was distilled under reduced pressure as above to give the desired product as a clear oil.

The 4-(hexafluoro-2-hydroxy isopropyl) styrene (HFHS) was prepared according to the method described by Pearce *et al.* [3] using a similar Grignard reaction as above with 4-chlorostyrene and hexafluoroacetone. The crude monomer was found by ^{1}H Nuclear Magnetic Resonance (NMR) to have spurious environments, which were attributed to THF complexing to the monomer. The crude product was washed with 10% NaOH solution to produce the sodium salt. This solution was then washed with chloroform to remove the THF. The caustic solution was then neutralised with

HCl and the resulting dense organic layer taken up in chloroform. The solvent was then removed by rotary evaporation and the monomer dried under vacuum using freeze-pump-thaw cycles until all solvent was removed. All monomers were characterised by infrared spectroscopy and ^{1}H NMR.

2.2. Copolymerisations

All copolymerisations were carried out under vacuum using toluene as the solvent and 0.4 mol% 2–2'-azobisisobutyronitrile (AIBN) as the initiator at 333 K. Polymerisations were terminated at low conversions by precipitation into a suitable non-solvent. Purification was typically achieved by two reprecipitations from toluene or dichloromethane into methanol or n-hexane. The polymers were dried for 72 h at 333 K in a vacuum oven followed by a further drying stage at 383 K for around 6 h.

Copolymers of styrene with VA and VTA were reduced with lithium aluminium hydride ($LiAlH_4$) using standard techniques to give the SHES and STFHS copolymers. The reduced copolymers were isolated and purified by repeated reprecipitations into n-hexane or methanol. The S-AS copolymer was hydrolysed in 1,4-dioxane using hydrazine hydrate as the hydrolytic agent according to previously reported conditions [17]. The hydrolysed copolymer was isolated and purified by repeated reprecipitations into petroleum ether (40–60°). The final copolymers were dried as described above. Copolymer compositions were determined as described previously [18, 19] and are represented in the text as SHS(SHFHS, STFHS or SHES)X, where X corresponds to the mole percentage of the co-monomer component in the copolymer.

Molar masses were measured by Gel Permeation Chromatography (GPC) using THF as the solvent. Molecular weights are reported with respect to PS standards. Details of the copolymers can be found in Table I. The PS used was a Pressure Chemical Company standard with M_n of 37,000.

2.3. Glass transition and enthalpy relaxation experiments

Glass transition (T_g) and enthalpy relaxation experiments were carried out on a Perkin-Elmer DSC-2, employing a single sample in the range 8–14 mg, with nitrogen as the purge gas. A heating rate of 20 K min^{-1} and a cooling rate of 40 K min^{-1} were employed throughout. Indium was used for temperature calibration and the data were evaluated with respect to sapphire as the heat capacity (C_p) standard.

The reported T_g values were the average of at least five scans and were the result of transforming the C_p data into enthalpy data according to the procedure of Richardson and Savill [20]. The point of intersection of the liquid and glassy enthalpy lines extrapolated into the transition region is taken to be the enthalpic T_g ($T_g(en)$) and is independent of scanning rate. The thermal history used in the ageing experiments has been described in detail previously [5].

2.4. Positron annihilation lifetime spectroscopy (PALS)

The PALS samples were prepared by moulding the polymers 50 K above the T_g under a pressure of 5 tonnes. The resultant samples were discs of 14 mm diameter having a thickness of 1–2 mm. Two discs were required to make the sample-source-sample sandwich.

The positron lifetime spectra were recorded using a conventional fast-slow coincidence method which has been described previously [21, 22]. The positron source used was ^{22}NaCl, sealed between two layers of Kapton (a polyimide, where virtually no Ps are formed, free e^+ has a lifetime of 382 ps) using epoxy adhesive. All PALS measurements were carried out at 293 K and each spectrum had approximately 10^6 counts. The tabulated results are the average of three consecutive runs.

The data processing used in the analysis of the spectra was developed by Kirkegaard, Pederson and Eldrup and is based on the PATFIT program [23]. It consists of POSITRONFIT and RESOLUTION fitting programs. Benzophenone was used for calculating the resolution of the instrument since it has a well defined single lifetime of 331 ps. The results from the RESOLUTION program were used as input parameters in the analysis of the unknown spectrum in POSITRONFIT. This is a least squares program which attempts to fit a lifetime (τ) and intensity (I) to each of the exponentials making up the spectrum. The results in this study are from fixed analysis where only the short component was fixed ($\tau_1 = 0.125$ ns) and the intensities, $I_3 : I_1$, constrained at a ratio of 3:1.

2.5. Fourier transform infrared spectroscopy (FTIR)

All infrared spectra were recorded on a Perkin Elmer RX FTIR spectrometer. The copolymers were cast from 1 wt% solutions in THF onto NaCl disks and dried

TABLE I Characterisation of the copolymers

Sample	M_n (kg mole^{-1}) [PS equiv]	M_w/M_n	T_g (en) (K)	ΔT (K)	ΔC_p (J K^{-1}g^{-1})	τ_3 (ns)	I_3 (%)	$\tau_3^3 I_3$ (ns^3%)
PS	37	1.1	374.1	4.6	0.283	2.00 ± 0.01	37.8 ± 0.3	307.1
SHES21	63	1.7	378.7	9.6	0.308	1.90 ± 0.02	26.0 ± 0.3	178.3
STFHS22	62	1.6	387.3	6.5	0.305	1.93 ± 0.03	23.0 ± 0.4	165.3
SHS22	93	1.5	399.9	5.4	0.338	1.85 ± 0.01	23.6 ± 0.2	149.4
SHFHS25	79	1.7	386.5	6.4	0.108	2.16 ± 0.02	24.4 ± 0.3	245.9

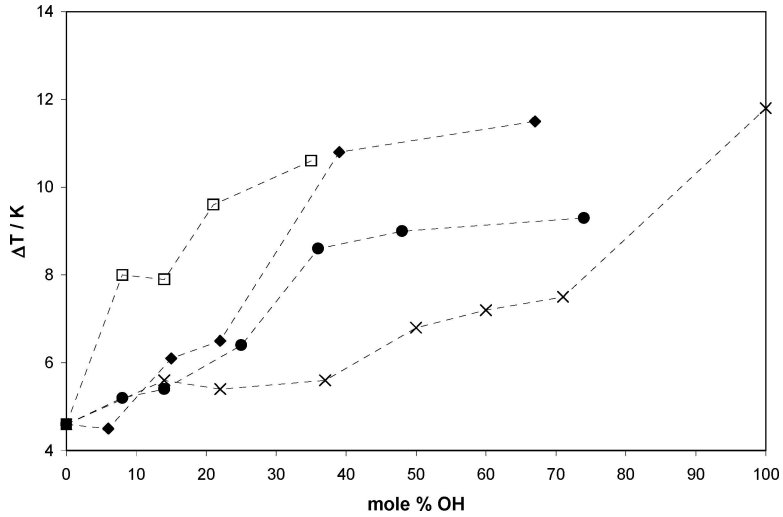

Figure 2 Dependence of glass transition width (ΔT) on copolymer composition for SHES21 (□), STFHS22 (♦), SHS22 (X) and SHFHS25 (●). Lines are intended as a guide for the eye.

under a high powered lamp prior to use. The SHFHS copolymer, however, was run as a KBr disk. Resolution of the instrument was set at 4 cm^{-1} and 64 scans were recorded.

3. Results and discussion

3.1. The glass transition

The enthalpic T_g, T_g width (ΔT) and heat capacity difference, ΔC_p, are shown in Table I. Copolymerisation results in an increase in T_g and broadening of ΔT with respect to PS. This can be attributed to the presence of hydrogen bonding groups and increases in chain rigidity in the copolymers.

Shown in Fig. 2 are plots of ΔT versus mol% modified co-monomer for a *complete* series of the copolymers. The level of microheterogeneity can be judged by the magnitude of ΔT and to a first approximation appears to increase in the order SHS < SHFHS < STFHS < SHES. The SHS copolymers possessed the lowest values of ΔT and this was thought to be a reflection of the ability of HS units to pack more efficiently and be in the correct steric configuration for hydrogen bonding. This would in turn result in the presence of fewer microenvironments as reflected by the low ΔT. Although SHFHS copolymers have the ability to form the strongest hydrogen bonds when blended with polymers containing a proton acceptor, such as PVME [4], the configuration of the bulky HFHS, appears to limit the amount of self-associated hydrogen bonding possible.

The quantity ΔC_p can be associated with the change of degrees of freedom in the glass transition region resulting from free volume changes [24]. For the SHS, STFHS and SHES copolymers in this study, values of ΔC_p were quite similar and were larger than that of PS. Generally a low ΔC_p reflects the fact that the number of accessible conformations is quite limited even at high temperature [25]. Indeed, the lowest value was measured for SHFHS25 and it was thought to be related to the inherent chain rigidity of this copolymer originating from the bulky HFHS group and its distribution along the copolymer chain.

3.2. Infrared spectroscopy

Infrared spectra of the copolymers were recorded at ambient temperature to see if we could gain a qualitative insight into the nature of hydrogen bonding in the copolymers. The SHS, SHES and STFHS copolymers all displayed distinctive hydroxyl stretching bands (see Fig. 3). The hydroxyl region of these copolymers exhibited both a free hydroxyl band (~3550 cm^{-1}) and a self-associated band due to intra- and inter-chain self-associations of hydroxyl groups (between 3600–3100 cm^{-1}). The self-associated band moved to lower wavenumbers in the order SHES21 (~3404 cm^{-1}) > STFHS22 (~3394 cm^{-1}) > SHS22 (~3364 cm^{-1}) suggesting an increase in the strength of the hydrogen bond in this order.

The situation for the SHFHS copolymer was more complicated than merely a simple equilibrium between free and self-associated environments [4]. Due to the fact that the SHFHS copolymer was prepared as a KBr disk, there was some scattering in the data and this obscured the free hydroxyl vibration at ~3600 cm^{-1}. The major hydroxyl environment was located at ~3516 cm^{-1} but a further environment was observed at lower wavenumbers (between 3300–3100 cm^{-1}). Dashed lines have been added to highlight these regions. In the SHFHS copolymer, there is the possibility of the hydroxyl group associating with a fluorine atom [4]. This has been discussed in more detail elsewhere [26]. Such additional interactions are likely to complicate the structure even further. The infrared data suggest that the intermolecular hydrogen bonding strength in the SHFHS copolymer is weaker in comparison with the other copolymer systems.

3.3. PALS

The PALS data at 293 K for the copolymers are given in Table I. Although the measurements were carried out at lower temperatures than those used for ageing, it was thought that the measurements would provide a comparison of the free volume properties of the copolymers.

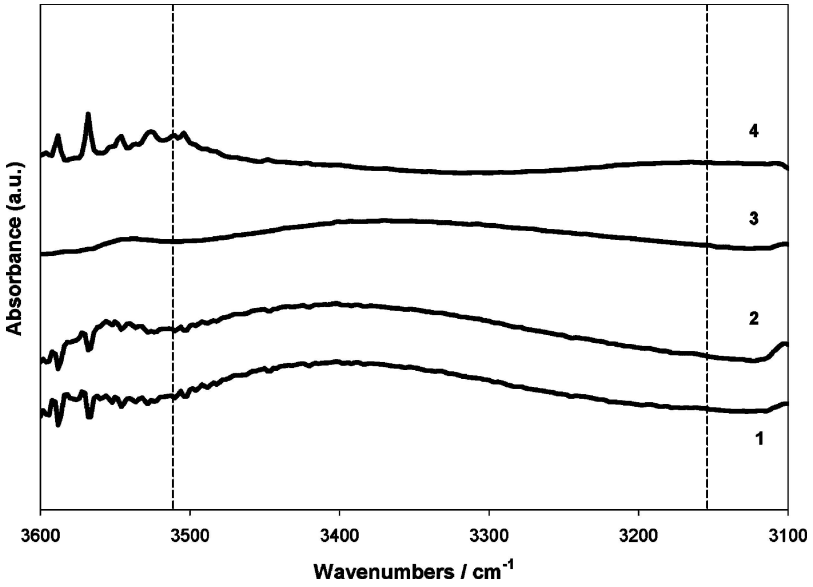

Figure 3 FTIR spectra in the hydroxyl stretching region from 3100 to 3600 cm^{-1} for SHES21 (1), STFHS22 (2), SHS22 (3) and SHFHS25 (4). For clarity, the spectra are shifted on the vertical axis.

For SHES21, STFHS22 and SHS22, the oPs lifetime and intensity decreased relative to PS. This reduction in free volume hole size (τ_3) could be indicative of the presence of hydrogen bonds in these copolymers, which are effectively acting as crosslinks. There will be a balance between the disruption of chain packing resulting from the introduction of the co-monomer component and the order imparted due to the formation of hydrogen bonds, and in these copolymers the latter effect is likely to be important.

In contrast, for SHFHS25 it is probably the former effect that is dominating resulting in a larger oPs lifetime and the weaker intermolecular hydrogen bonding interactions as observed by infrared spectroscopy. As we have noted previously [26], it is not unreasonable to expect a larger free volume for SHFHS containing 25 mol% of HFHS given the likely changes in chain packing due to presence of the rigid and bulky co-monomer. Effects due to disruption of chain packing in copolymers have been observed in other copolymer systems using PALS [27, 28]. It is also necessary to consider that the co-monomer sequence distribution will have an impact on the local packing of repeat units in the copolymers [29].

The I_3 value measured for PS was close to 40%, but I_3 values for the copolymers were lower, and relatively comparable. It would be instinctive to suggest that the reduction was due entirely to changes in free volume distributions resulting from the presence of hydrogen bonds. However, I_3 has to be used cautiously as there is the possibility of positron chemistry and inductive processes occurring [30]. Nevertheless, analysis of the shorter lifetime components provided us with confidence that positron chemistry effects were negligible in our samples.

The quantity, $\tau_3^3 I_3$, is reported to be proportional to the fractional free volume as described by a simple spherical cavity model, and is found to be a good indicator of free volume characteristics in polymers [31]. The apparent fractional free volume was found to decrease in the order PS > SHFHS25 > SHES21 > STFHS22 > SHS22. This order roughly correlates with the hydrogen bond strength as estimated (qualitatively) from the infrared measurements.

3.4. Enthalpy relaxation

Enthalpy relaxation experiments were performed on each of the copolymers at 5, 10 and 15 K below T_g. Shown in Fig. 4 are typical heat capacity curves for the SHS copolymer at 15 K below T_g. The effect of ageing was to increase progressively the size and peak maximum of the endothermic recovery peak. This behaviour was typical of all of the copolymers studied.

Fig. 5a–c shows the C_p curve of the materials after ageing for 500 minutes at 15, 10 and 5 K below T_g, respectively. This enables us to qualitatively compare the differences in enthalpic recovery between PS and the copolymers. At all undercoolings, the enthalpy recovery peak for pure PS is considerably sharper than any of the copolymers. Incorporation of the different co-monomers, however, greatly changes the shape and peak position of the enthalpy recovery peak. The SHS copolymer exhibited the narrowest peak of all the copolymers, and this was located at the highest temperatures as expected. For the SHS copolymer, it is most likely that the hydroxyl groups have easily ordered together through self-association to create favourable domains.

Also worthy of comment is the fact that the peaks for SHES were much broader than the other systems. This was thought to reflect the increased heterogeneity as confirmed by ΔT and implies that energy is released over a much wider range of temperature in this copolymer. It should be noted, however, that the breadth of the enthalpy recovery peaks for all of the samples increased when aged at 5 K below T_g. Most striking was the enthalpy relaxation peaks for SHFHS, which clearly show this copolymer is less able to release enthalpy

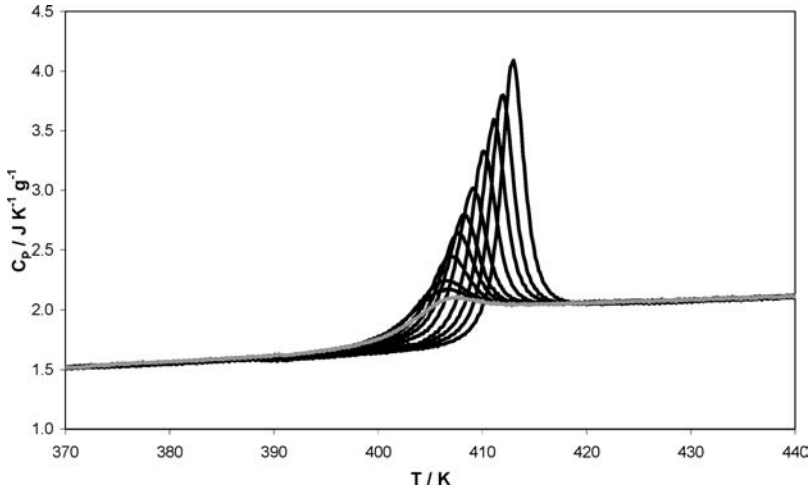

Figure 4 Heat capacity curves for SHS22 aged 15 K below T_g for increasing ageing periods reference scan (grey curve), 5, 10, 30, 60, 100, 200, 500, 1000, 2000 and 5000 min).

compared with the other systems, most probably due to the increased rigidity of the chains due to the HFHS segments.

The ageing data were fitted to the CF model and the parameters are given in Tables II–VI. The plots of ΔH (T_a, t_a) versus log (t_a) are shown in Figs. 6a–e. The plots include the theoretical curves obtained from the CF model. Data for PS has been included to serve as a comparison.

The first point to note is that generally the enthalpy lost after a given ageing time increases as T_a decreases. This is what we would expect since the distance between the glassy and extrapolated liquid enthalpy lines increases as the system progresses deeper into the glassy region.

The values of log (t_c) were plotted against undercooling ($T_g - T_a$) for each of the copolymers (Fig. 7). This parameter can give us an idea of the kinetics of the process, in that a low value indicates a fast relaxation process and vice versa. In general, the ageing process is slower with decreasing T_a, since the motion of relaxing elements is more restricted as we lower the temperature below T_g, as one would expect.

Clearly, incorporation of a co-monomer capable of hydrogen bonding alters the kinetics of ageing, but in an unpredictable manner. To a first approximation, the introduction of hydrogen bonds appears to slow the relaxation compared with PS. At temperatures close to T_g, the SHES copolymer relaxes most slowly, whilst the SHS copolymer relaxes most quickly. However, at the lowest undercooling, the copolymers all relax slowly and with similar rates. Interestingly, SHES21 relaxed slowly at all ageing temperatures investigated.

The β parameter gives an idea of the degree of non-exponentiality of the relaxation. A β value of unity reflects an essentially exponential process with a narrow distribution of relaxation times. The variation in β was not predictable and so it is not desirable to make any conclusions based on this parameter. In fact, for accurate predictions of the CF parameters, the $\Delta H(T_a, t_a)$ versus log (t_a) data should pass through an inflection

TABLE II CF parameters for PS

T_a (K)	$T_g - T_a$ (K)	$\Delta H_\infty(T_a)$ (J g^{-1})	log (t_c) (min)	β	$\Delta H_{max}(T_a)$ (J g^{-1})
358	16	2.05	2.05	0.39	4.79
363	11	1.93	1.71	0.44	3.27
368	6	1.11	0.91	0.47	1.85

TABLE III CF parameters for SHES21

T_a (K)	$T_g - T_a$ (K)	$\Delta H_\infty(T_a)$ (J g^{-1})	log (t_c) (min)	β	$\Delta H_{max}(T_a)$ (J g^{-1})
364	15	3.38	2.58	0.31	7.37
369	10	3.14	2.42	0.36	5.43
374	5	2.70	2.17	0.37	3.56

TABLE IV CF parameters for STFHS22

T_a (K)	$T_g - T_a$ (K)	$\Delta H_\infty(T_a)$ (J g^{-1})	log (t_c) (min)	β	$\Delta H_{max}(T_a)$ (J g^{-1})
372	15	2.96	2.73	0.31	4.82
377	10	1.96	1.92	0.36	3.21
382	5	1.06	1.11	0.29	1.69

TABLE V CF parameters for SHS22

T_a (K)	$T_g - T_a$ (K)	$\Delta H_\infty(T_a)$ (J g^{-1})	log (t_c) (min)	β	$\Delta H_{max}(T_a)$ (J g^{-1})
385	15	2.82	2.51	0.33	5.66
390	10	2.13	1.91	0.37	3.77
395	5	0.92	0.65	0.55	2.02

TABLE VI CF parameters for SHFHS25

T_a (K)	$T_g - T_a$ (K)	$\Delta H_\infty(T_a)$ (J g^{-1})	log (t_c) (min)	β	$\Delta H_{max}(T_a)$ (J g^{-1})
371.5	15	0.87	2.42	0.34	2.75
376.5	10	0.89	2.47	0.30	1.93
381.5	5	0.43	1.21	0.52	1.21

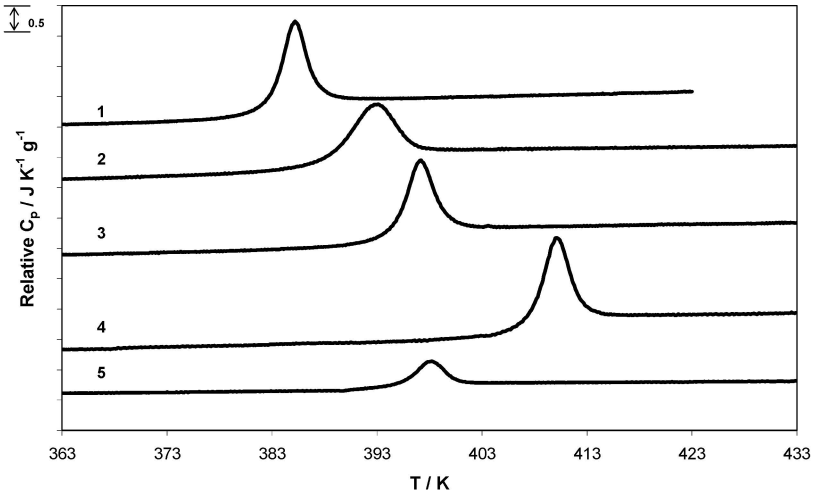

(a)

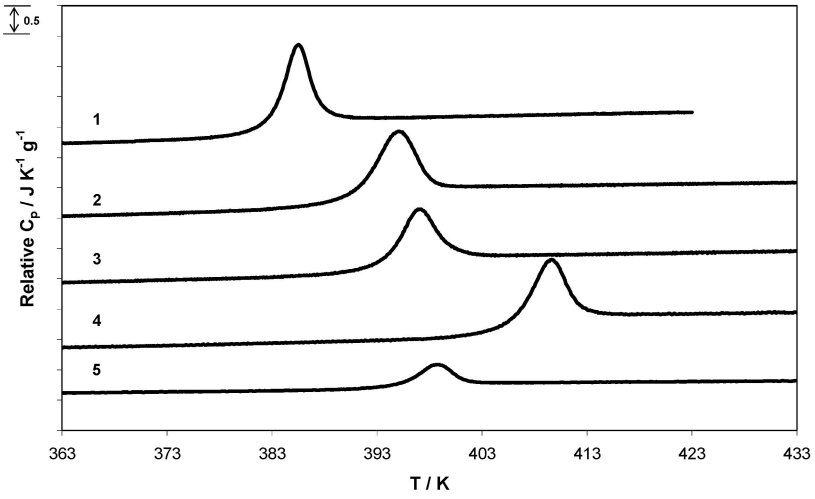

(b)

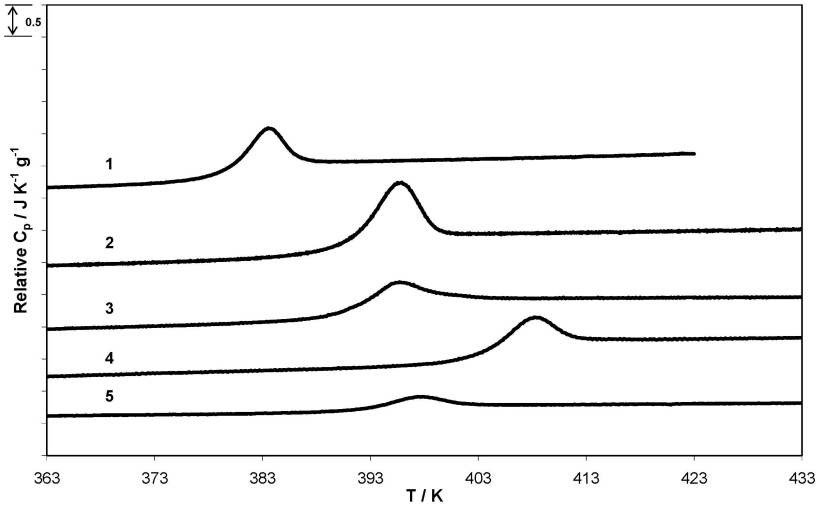

(c)

Figure 5 Heat capacity curves for (1) PS, (2) SHES21, (3) STFHS22, (4) SHS22 and (5) SHFHS25 aged for 500 min at (a) 15 K below T_g , (b) 10 K below T_g and (c) 5 K below T_g. Curves have been displaced vertically for clarity.

point, however, this was not always the case, especially at the lowest T_a. An estimated error in the β parameter of around 5% was obtained by performing curve fitting tests on a system with a well-defined inflection point. Such an error would not account for the differences in β for a particular copolymer at different ageing temperatures.

Brunacci *et al.* [7] questioned whether β and log (t_c) parameters could be reasonably used to draw comparisons between various para-substituted polystyrenes. They argued whether β and log (t_c) were "pure" kinetic parameters, which may or may not be structure specific. They found that the β and log (t_c) showed no correlation with substituent structure in their

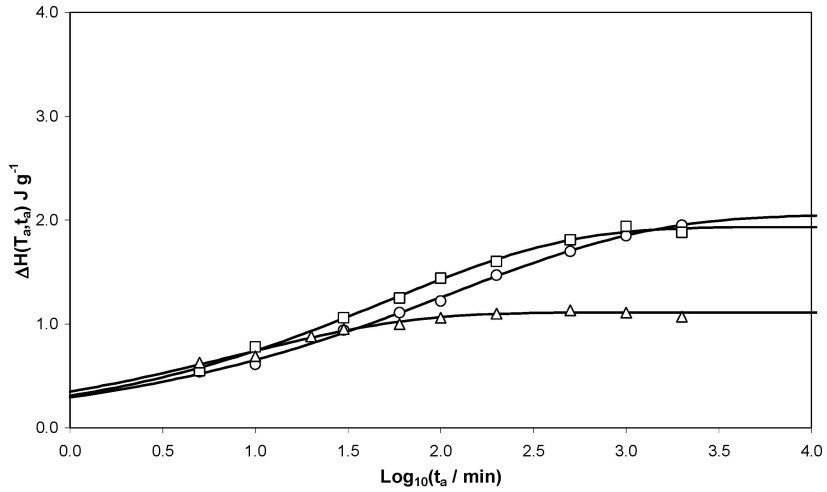

(a)

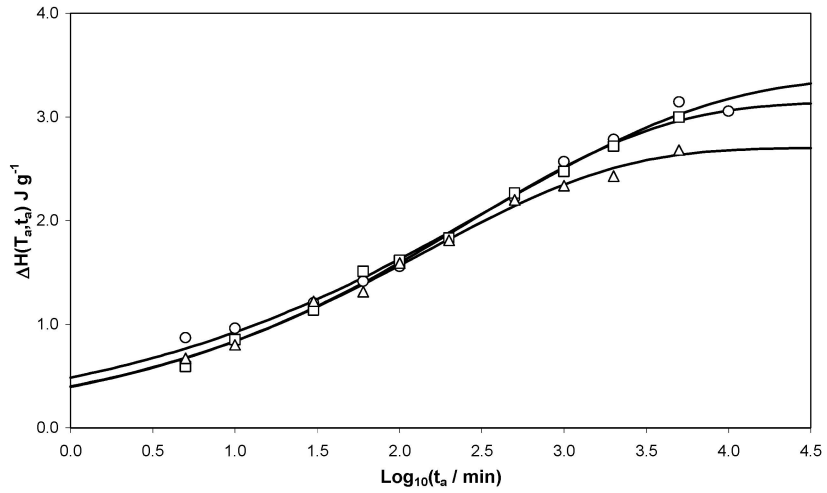

(b)

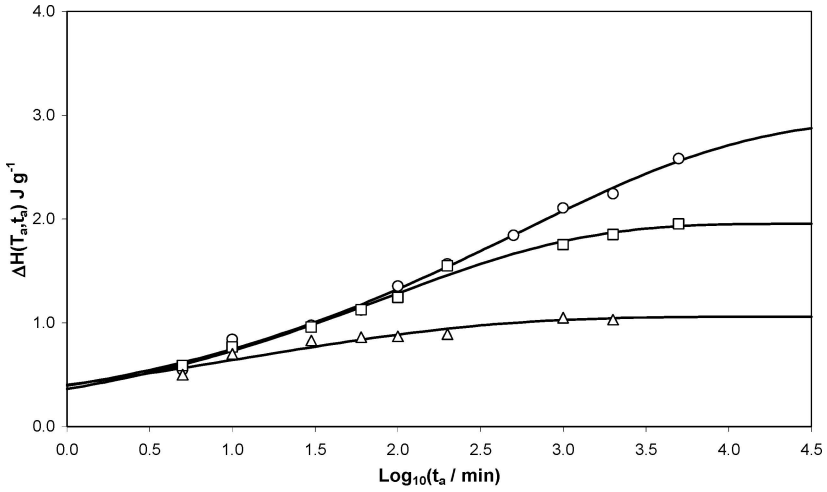

(c)

Figure 6 Enthalpy relaxation data for: (a) PS at $T_a = 358$ K (○), 363 K (□) and 368 K (△); (b) SHES21 at $T_a = 364$ K (○), 369 K (□) and 374 K (△); (c) STFHS22 at $T_a = 372$ K (○), 377 K (□) and 382 K (△); (d) SHS22 at $T_a = 385$ K (○), 390 K (□) and 395 K (△) and (e) SHFHS25 at $T_a = 371.5$ K (○), 376.5 K (□) and 381.5 K (△). Solid lines are fits to the experimental data using the CF equation. (*Continued*)

series of polystyrenes and, with the exception of poly(4-hydroxystyrene) (PHS), the total relaxable enthalpy $\Delta H_\infty(T_a)$ was broadly similar for all the samples. It was suggested, however, that $\Delta H_\infty(T_a)$ was a promising parameter for rationalising ageing data because it should reflect a distinct thermodynamic condition and should be more amenable to prediction from a model of the glassy state.

With this is mind, the variation of $\Delta H_\infty(T_a)$ with $(T_g - T_a)$ for the copolymers has been plotted in Fig. 8. In contrast with the kinetic data, this parameter shows clear variations between the various copolymers. The

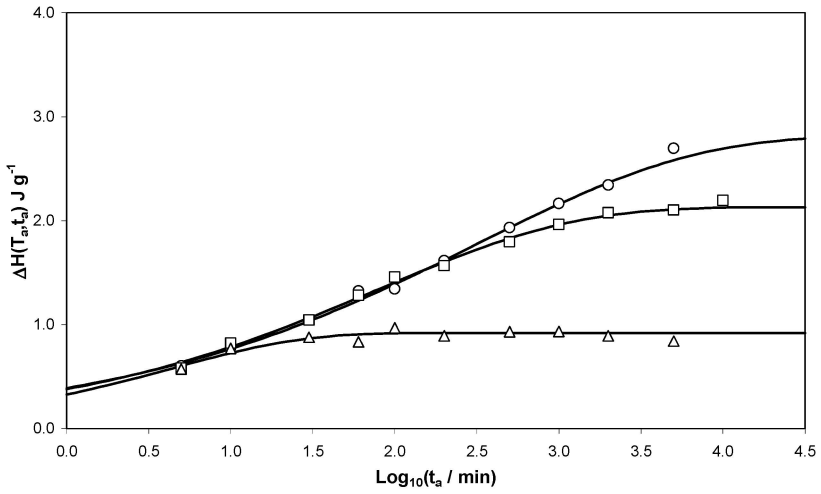

(d)

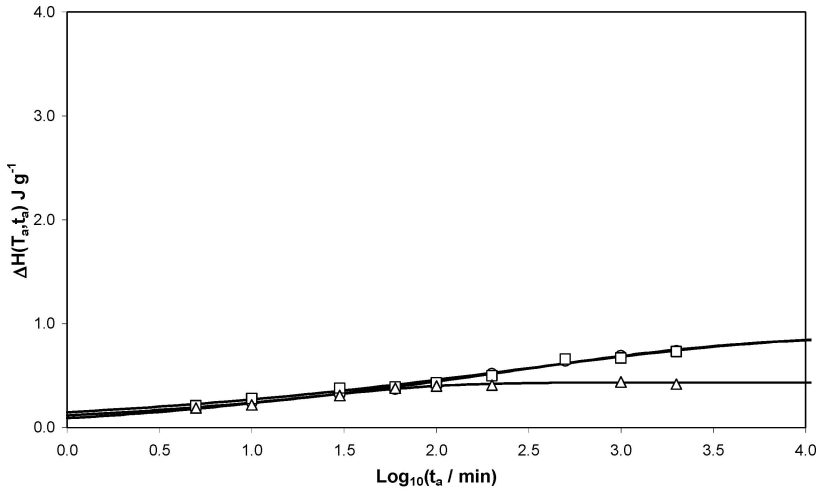

(e)

Figure 6 (*Continued*)

lowest equilibrium enthalpy values were found at all ageing temperatures for SHFHS25. The highest values at all ageing temperatures were measured for SHES21, and it is interesting to note that the relaxation kinetics were slow for this copolymer. Higher equilibrium enthalpy values could suggest that the hydroxyl groups find themselves in a highly unfavourable environment and are able to release extra energy through structural rearrangements to achieve a more favourable structure.

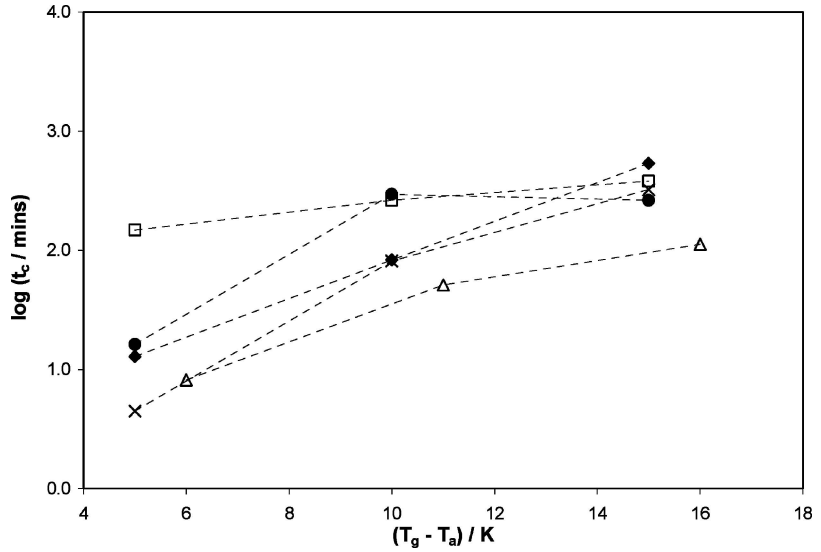

Figure 7 Variation of log (t_c) with ($T_g - T_a$) for PS (△), SHES21 (□), STFHS22 (♦), SHS22 (X) and SHFHS25 (●). Lines are intended as a guide for the eye.

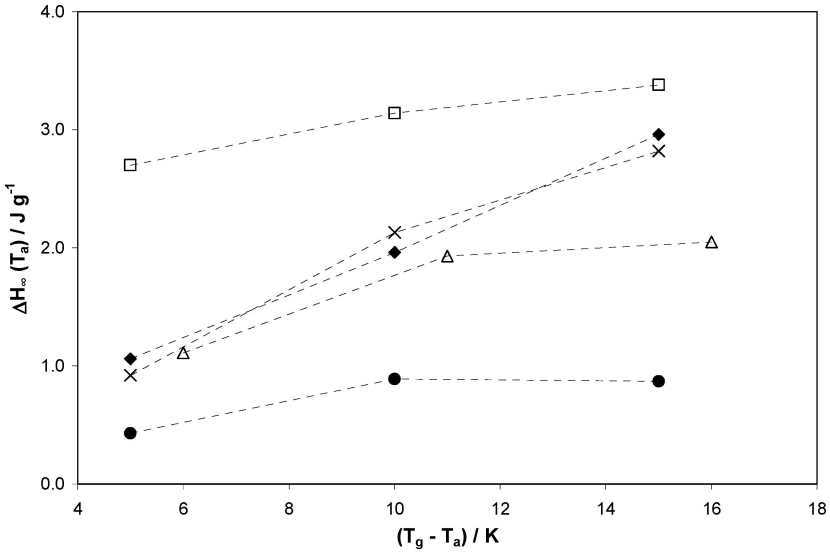

Figure 8 Variation of $\Delta H_\infty(T_a)$ with $(T_g - T_a)$ for PS (△), SHES21 (□), STFHS22 (♦), SHS22 (X) and SHFHS25 (●). Lines are intended as a guide for the eye.

It is of interest to note the small magnitude of ΔC_p and $\Delta H(T_a, t_a)$ for the SHFHS copolymer. The fact that this copolymer is not able to release as much enthalpy as the other systems links us back to the inherent rigidity and co-monomer distribution of this copolymer. The increased free volume for this copolymer cannot be used to account for its enthalpy relaxation behaviour.

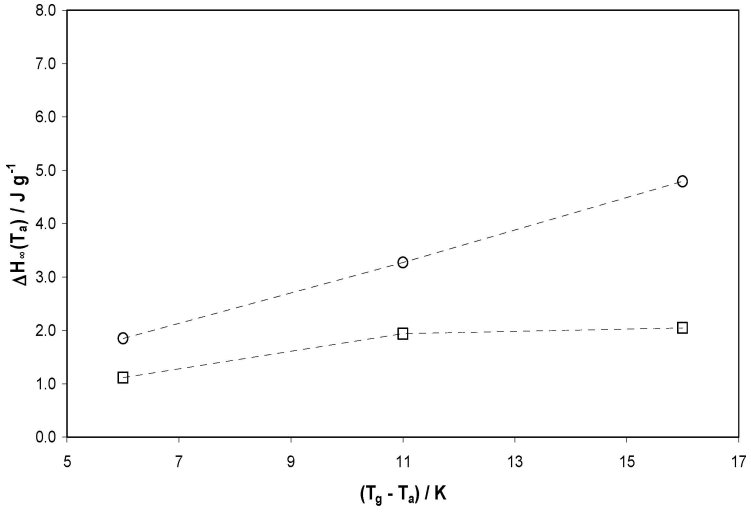

(a)

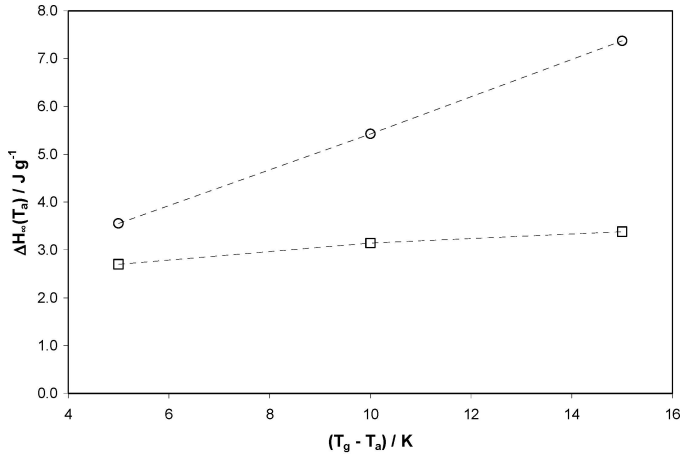

(b)

Figure 9 Comparison of $\Delta H_{max}(T_a)$ (○) and $\Delta H_\infty(T_a)$ (□) for (a) PS; (b) SHES21; (c) STFHS22; (d) SHS and (e) SHFHS25. Lines are a guide for the eye. (*Continued*)

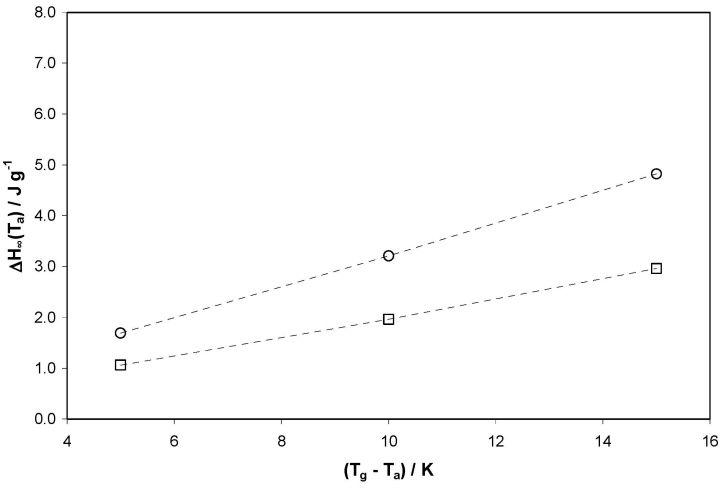

(c)

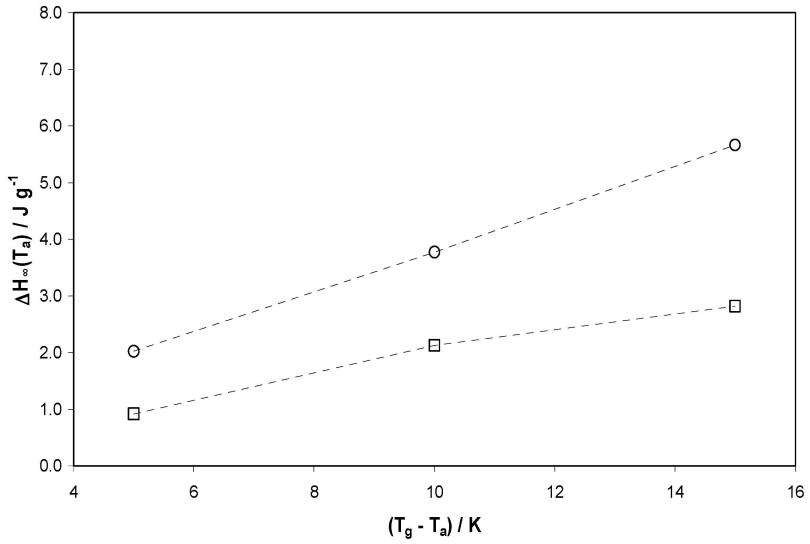

(d)

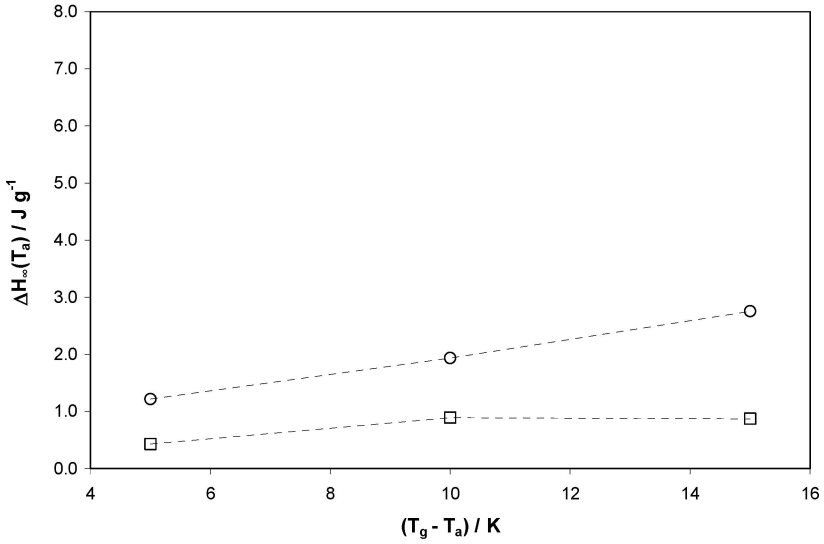

(e)

Figure 9 (*Continued*)

The equilibrium enthalpy difference ($\Delta H_\infty(T_a)$) can be compared with the calculated maximum enthalpy lost on relaxing to the extrapolated liquid enthalpy curve ($\Delta H_{max}(T_a)$). This has been shown in graphical form for clarity (Figs 9a–e). The $\Delta H_{max}(T_a)$ values were determined from the C_p versus temperature plots of unaged (reference) material. Integrations were performed on the region between the curve and the linear extrapolation of its liquid part to below T_g using the ageing temperatures as integration limits. The $\Delta H_{max}(T_a)$

which can be lost on ageing was found to be higher than $\Delta H_\infty(T_a)$ as calculated by the CF equation in every case. This result has been consistently noted in our previous investigations [5, 8, 11]. This is an important point to consider because many other models of enthalpy relaxation assume that $\Delta H_\infty(T_a)$ is equal to $\Delta H_{max}(T_a)$. Equilibrium enthalpy values for SHES21 seem to be farther below the calculated maximum enthalpy than any of the other copolymers, which again could be linked to the increased heterogeneity in this system and its reduced ability to form hydrogen bonds. For all of the polymers studied, $\Delta H_\infty(T_a)$ approaches $\Delta H_{max}(T_a)$ when T_a is close to T_g.

As noted by Cameron *et al*. [8, 11], the presence of chain entanglements and random coil formations in the glassy state, prevent the possibility of perfect packing. If we consider that physical ageing occurs due to the driving force of an amorphous polymer in the non-equilibrium state to reach a state of equilibrium, then there could be a physical limit to the process of chain packing and ordering. That is, as the free volume reduces with ageing time, there will come a stage where no further densification is possible, as represented by $\Delta H_\infty(T_a)$ values falling short of $\Delta H_{max}(T_a)$ values.

4. Concluding remarks

Infrared spectroscopy revealed that in the SHES, STFHS and SHS copolymers (listed in order of increasing hydrogen bond strength), the hydroxyl groups participated in the formation of self-associated hydrogen bonds with some free hydroxyls remaining. A more complex situation was observed for the SHFHS copolymer than just a simple equilibrium between free and self-associated environments. A further environment was noted at lower wavenumbers, which was attributed to an interaction between a fluorine atom and a hydroxyl group. The infrared data suggested a different hierarchy in hydrogen bond strength from that measured previously for PVME blends of these copolymers [4].

Enthalpy relaxation experiments on copolymers with varying hydrogen bond strengths were carried out at different temperatures below T_g, and provided useful long–term ageing data from short-term tests. Examination of the experimental heat capacity curves was useful for qualitatively assessing the differences in enthalpy relaxation of the copolymers and we were able to make links with heterogeneity and chain rigidity.

The CF model was applied successfully. Generally, all of the copolymers relaxed more slowly than PS, especially at the lower undercoolings. This was indicative of the restrictions of the relaxation processes caused by the presence of hydrogen bonds; however, the effects of rigidity and the disorder imparted by incorporating the co-monomer component also had to be considered.

Most informative was the enthalpic parameter, which changed significantly for each of the copolymers. Unusually low values of $\Delta H_\infty(T_a)$ were obtained for the SHFHS copolymer; whereas, the highest values were measured for the SHES copolymer. Higher equilibrium enthalpy values could suggest that the hydroxyl groups are in a highly unfavourable (non-polar) environment and are more able to release extra energy through structural rearrangements to achieve a more favourable structure.

Comparison of $\Delta H_\infty(T_a)$ values with the calculated maximum enthalpy on relaxing to the equilibrium liquid enthalpy line ($\Delta H_{max}(T_a)$) showed that none of the copolymers achieved this theoretical equilibrium state, and that the SHES copolymer in particular equilibrates at significantly higher enthalpy values.

At the copolymer compositions used in this study, the oPs lifetime values were believed to reflect changes in molecular size and hence packing effects due to the different substituents on the macromolecular chains. The experimental evidence suggests that free volume effects are less important than effects such as intrinsic chain rigidity, the extent and type of hydrogen bonds present and the randomness of co-monomer distribution in the polymer chains.

Acknowledgements

Financial support for this work came from the EPSRC. For assistance with the PALS measurements the authors would like to thank Dr. David Hayward and Mr. John Carruthers from Strathclyde University. E-AM would also like to acknowledge Dr. Iain McEwen and Dr. Roderick Ferguson for their guidance with regards to the enthalpy relaxation experiments.

References

1. J. M. HUTCHINSON, *Prog. Polym. Sci.* **20** (1995) 703.
2. L. C. E. STRUIK, "Physical Ageing in Polymers and Other Materials" Elsevier, Amsterdam (1978).
3. E. M. PEARCE, T. K. KWEI and B. Y. MIN, *J. Macromol. Sci. Chem.* A **21** (1984) 1181.
4. J. M. G. COWIE, B. G. DEVLIN and I. J. MCEWEN, *Polymer* **34** (1993) 4130.
5. J. M. G. COWIE and R. FERGUSON, *ibid.* **34** (1993) 2135.
6. J. M. G. COWIE, S. HARRIS and I. J. MCEWEN, *J. Polym. Sci. Phys. Ed.* **35** (1997) 1107.
7. A. BRUNACCI, J. M. G. COWIE, R. FERGUSON and I. J. MCEWEN, *Polymer* **38** (1997) 865.
8. N. R. CAMERON, J. M. G. COWIE, R. FERGUSON and I. MCEWAN, *ibid.* **41** (2000) 7255.
9. J. M. G. COWIE and R. FERGUSON, *Macromolecules* **22** (1989) 2312.
10. E.-A. MCGONIGLE, J. M. G. COWIE, V. ARRIGHI and R. A. PETHRICK, submitted to Polymer.
11. N. R. CAMERON, J. M. G. COWIE, R. FERGUSON and I. MCEWAN, *Polymer* **42** (2001) 6991.
12. J. L. GÓMEZ RIBELLES and M. MONLEÓN PRADAS, *Macromolecules* **28** (1995) 5867.
13. A. BRUNACCI, J. M. G. COWIE, R. FERGUSON, J. L. GÓMEZ RIBELLES and A. VIDAURRE GARAYO, *ibid.* **29** (1996) 7976.
14. D. M. BIGG, *Polym. Engng. Sci.* **36** (1996) 737.
15. W. O. KENYON and G. P. WAUGH, *J. Polym. Sci.* **32** (1958) 83.
16. C. CHENG and E. M. PEARCE, *J. Polym. Sci. Polym. Chem. Ed.* **18** (1980) 1651.
17. R. ARSHADY, G. W. KENNER and A. LEDWITH, *J. Polym. Sci. Polym. Chem.* **12** (1974) 2017.
18. G. LI, J. M. G. COWIE and V. ARRIGHI, *J. Appl. Polym. Sci.* **74** (1999) 639.

19. J. M. G. COWIE and A. A. N. REILLY, *Polymer* **33** (1992) 4814.
20. M. J. RICHARDSON and N. G. SAVILL, *ibid.* **16** (1975) 753.
21. R. A. PETHRICK, F. M. JACOBSEN, O. E. MOGENSEN and M. ELDRUP, *J. Chem. Soc., Faraday II* **76** (1980) 225.
22. W. J. DAVIES and R. A. PETHRICK, *Eur. Polym. J.* **30** (1994) 1289.
23. P. KIRKEGAARD, M. ELDRUP, O. E. MOGENSEN and N. PEDERSEN, *Comp. Phys. Commun.* **23** (1981) 307.
24. S. N. CASSU and M. I. FELISBERTI, *Polymer* **38** (1997) 3907.
25. G. LEVITA and L. C. E. STRUIK, *ibid.* **24** (1983) 1071.
26. E.-A. MCGONIGLE, J. M. G. COWIE, V. ARRIGHI and R. A. PETHRICK, to be submitted for publication.
27. C. WÄSTLUND, H. BERNSTSSON and F. H. J. MAURER, *Macromolecules* **31** (1998) 3322.
28. E.-A. MCGONIGLE, J. J. LIGGAT, R. A. PETHRICK, S. D. JENKINS, J. H. DALY and D. HAYWARD, *Polymer* **42** (2001) 2413.
29. M. K. GRAY, H. ZHOU, S. T. NGUYEN and J. M. TORKELSON, *ibid.* **45** (2004) 4777.
30. R. A. PETHRICK, *Prog. Polym. Sci.* **22** (1997) 1.
31. A. J. HILL, S. WEINHOLD, G. M. STACK and M. R. TANT, *Eur. Polym. J.* **32** (1996) 843.

Received 8 November
and accepted 21 December 2004